Pacific Graphics (2013)
B. Levy, X. Tong, and K. Yin (Editors)

Modeling Large Scale Clouds from Satellite Images

Chunqiang Yuan Xiaohui Liang Shiyu Hao Guang Yang

State Key Laboratory of Virtual Reality Technology and Systems, Beihang University

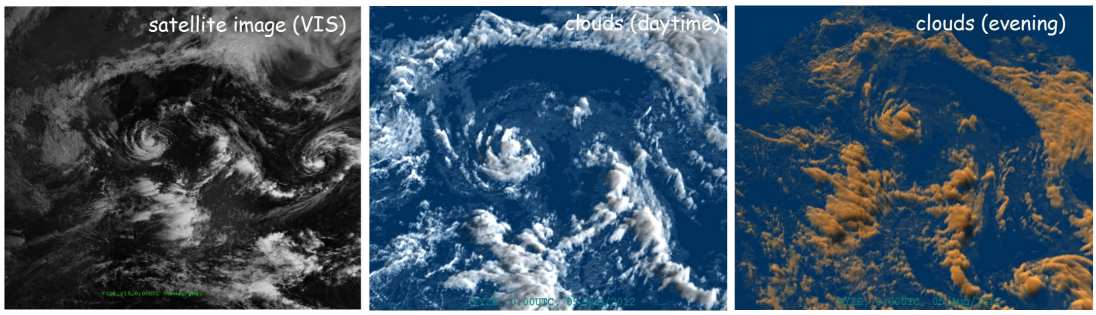

Figure 1: *Large scale clouds are generated from multi-spectral satellite images.*

Abstract

Visualization of satellite cloud images plays an important role in atmosphere analysis and weather prediction. However, reconstruction of meaningful 3D clouds is a challenging problem due to the 2D nature of the input data. In this paper, we present a new method for modeling large scale clouds based on cloud property retrieval theory. In contrast with previous methods, the proposed one is more physical and focuses on the geometric structures of clouds. Image pixels are first divided into cloudlessness, water cloud, ice cloud, and thin cirrus cloud in terms of spectral characteristics. Then, the top height, geometry thickness and extinction volume of the cloud are generated by applying different spectral combinations of images. Finally, clouds are rendered with various light directions or view directions. The results show that the proposed method can not only yield realistic clouds, but also approximate actual clouds, thus being useful for time critical applications.

Categories and Subject Descriptors (according to ACM CCS): I.3.m [Computer Graphics]: Miscellaneous—

1. Introduction

Clouds occupy more than 60% of the sky at any given time and are the main regulators of weather and climate. Visualization of large scale clouds are of importance to weather forecasting, especially to very short range forecasts or even nowcasting. As primary monitors of earth-scale clouds, meteorological satellites, such as METEOSAT, GOES, FY2E, MTSAT, etc., collect invaluable cloud-related information via remote sensors and transmit the information back to the ground in the form of multi-spectral satellite images every thirty or fifteen minutes. These images are an important source for analyzing clouds, and can also provide graphics researchers with new opportunities to model clouds.

For weather forecasting and atmospheric research, contours, vectors, and height field are usually used to visualize the cloud properties estimated from satellite images. However, due to the nature of color mapping, it is generally difficult to give a good presentation of the 3D climate environment by these techniques, especially when multiple views or sun directions are considered for a same cloud scene. In the graphics community, a few methods have been proposed for producing realistic looking densities of clouds but are not guaranteed to be physically valid. The resulting clouds

DOI: 10.2312/PE.PG.PG2013short.047-052

are similar to those in the input images but are not actual presentation of cloud characteristics, such as the height and thickness. Hence, these methods may not be suitable for analyzing the evolution of clouds although they can generate visually appealing cloud scenes.

To address these problems, we propose a method to visualize large scale clouds from multi-spectral satellite images. Specific spectral images are used to compute cloud properties. Based on these properties, we generate the geometric shape and extinction volume of the cloud for rendering. Using the system, the weatherman can easily understand the structural changes of large scale clouds when continuous images are used. Fig. 1 shows that large scale clouds are generated from multi-spectral satellite images of FY2E(one of Chinese meteorological satellites). These images are in the Mercator projection and cover the large sea area.

2. Related work

Cloud modeling has received increasing attention in areas such as weather forecasting, flight simulation, and atmospheric research. Most mainstream methods utilize either a procedural approach or a physically based approach for cloud modeling. Procedural modeling, which is the most popular cloud modeling approach, includes methods based, for example, on textured ellipsoids [Gar85], noise functions [Ebe], and interactive designs [BN04, WBC08]. These methods can generate realistic clouds, but many parameters are required and must be determined by trial and error methods. To avoid the necessity of parameter setting, physically based cloud simulations have become a favorite among researchers. Miyazaki et al. [MYND01] modeled various types of clouds using a coupled-map lattice method. Harris et al. simulated cloud formation processes on graphics hardware [Har05]. Recently, Dobashi et al. proposed a method to control the simulation to generate desired shapes of cumulus clouds [DKNY08]. These physically based methods are primarily concerned with small scale scenes and usually used to create realistic clouds in artistic design community.

However, these two methods are both weak in simulating actual cloud scenes. In contrast, modeling clouds from real data can generate clouds closely related to the input data. Typical cloud related data includes satellite images [DNYO98, DYN09], images [DSY10, DIO*12], and numerical simulation data [REHL03]. Early, Dobashi et al. used a simplified single scattering model to inverse earth-scale clouds from infrared satellite images [DNYO98]. Recently, for rendering earth-scale clouds, they utilized an approximate scheme to construct the shapes of the clouds from infrared images [DYN09]. The goal behind both of these works is to produce realistic looking clouds, but not necessarily accurate ones. By contrast, our method is based on cloud property retrieval theory [KR04] and is thus more physically based in that multi-spectral images are jointly used to compute cloud geometry and extinction.

3. Cloud modeling from satellite images

3.1. Overview

In this proposed method, cloud properties are derived from five-spectral images provided by FY2E, including visible (VIS,0.55$\sim$ 0.90 μm), infrared (IR1,10.5$\sim$ 12.5 μm), split (IR2) , water-vapor (WV,6.3$\sim$ 7.6 μm), and mid-wave infrared (MWIR,3.5$\sim$ 4.0 μm). For each pixel (longitude, latitude), the first image records the reflectance $\Re_i$ indicating the ratio of the reflected intensity to the incident solar flux density, and the last four record the temperature T_i where the subscript i denotes the waveband.

The process of cloud modeling consists of four steps. First, image pixels are simply segmented into four types. Then, IR1 and WV images are combined to locate the cloud top height. After that, we use MWIR and VIS images to retrieve the geometric thickness and extinction for water and ice cloud pixels. For thin cirrus cloud pixels, the thickness and extinction are derived from the temperature dependent models. Finally, we generate a regular volume data and a particle system for rendering.

To make our method be feasible, four assumptions are used including the constant ground temperature at a fixed time (Sec. 3.2), the linear relationship between the temperature and the altitude(Eq. (1)), the homogeneous layer (Eq. (2)) and the width being equal to the length of ice crystal ((Eq. 4).

3.2. Pixel classification

The classification of image pixels is an essential first step in the retrieval of cloud parameters(e.g., the height and the thickness). Since the ground is warmer than the cloud, a pixel is cloudy if the temperature difference between the ground and the IR1 image is above a threshold (2.5K), otherwise the pixel is clear-sky. However, ground temperatures for some desolated places are almost inaccessible due to the sparse distribution of measuring instruments. Luckily, at a fixed time, the temperature of a given geographic location remains roughly constant over a period of a few days. Therefore, we take the maximum temperature at the same time during the period of the last 15 days as the ground temperature. When the sky remains cloudy for 15 days, the maximum temperature is lower than the actual temperatures. If the maximum temperature is lower than the average monthly temperatures of the sea(289K in August), we set the ground temperature to the average temperature.

Next, the cloud pixels is divided into water clouds, ice clouds, thin cirrus clouds in terms of the spectral characteristics of the clouds. When a pixel is covered by thin cirrus clouds, the temperature difference between IR1 and IR2 wavebands is remarkable while the difference is often less than 1K for clear sky [Ino87]. Therefore, a cloud pixel is labeled as thin cirrus cloud if the temperature difference is above a threshold (1.4K). For high clouds (ice

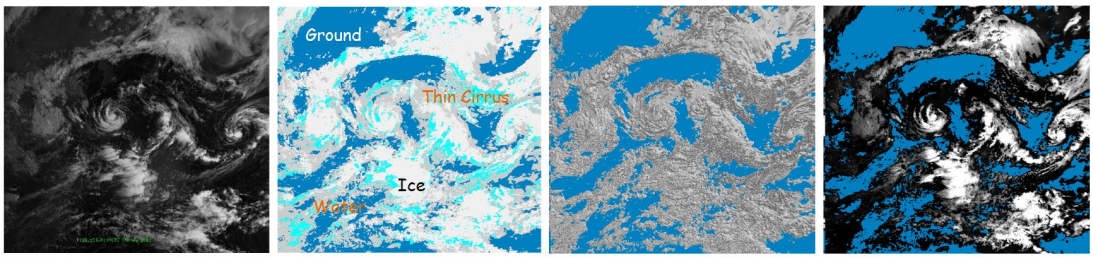

Figure 2: *(a) the input visible image. (b) pixel types. (c) the top of the cloud. (d) the distribution of estimated thickness.*

clouds), the WV image is closely associated with the IR1 image [XZYZ08]. In this sense, we use the slope of the scattergraph between the IR1 image and the WV image to discriminate ice clouds from water clouds. For each cloud pixel, we use 3×3 pixels to generate a linear fit of the scattergraph. If the slope $\frac{dT_{wv}}{dT_{ir1}}$ of the linear fit is less than 0.1, the cloud pixel is labeled as water cloud, otherwise as ice cloud. The classification result is shown in Fig. 2(b) where dark blue pixels denote the ground(clear-sky), white pixels indicate ice clouds, gray pixels represent water clouds and light blue pixels are thin cirrus clouds.

3.3. Cloud top height estimation

For optically thick clouds (water clouds and ice clouds), the ground infrared radiation is hardly sensed by the satellite. The measured temperature in IR1 image can be treated as the temperature at the top of the cloud. For the thin cirrus, the measured temperature is however usually higher than that of the cloud top due to the contribution of the infrared radiation from the ground. To derive the temperature of the thin cirrus, we use the bi-spectrum method proposed by Szejwach [Sze82] from the IR1 image and WV images.

Clouds usually occur in the troposphere layer. With the increase of the altitude, the temperature approximately decreases by 6.5K per 1km at the standard atmosphere. After the temperature of the cloud T_c is available, cloud top height CTH can be computed using the following equation:

$$CTH = H_0 + (T_{ir1}^g - T_c)/6.5 \tag{1}$$

where H_0 is the altitude of current pixel position, T_{ir1}^g the ground temperature in the IR1 waveband. The cloud top surface is presented in Fig. 2 (c).

3.4. Cloud thickness and extinction computation

The optical thickness τ is the integral of the extinction coefficient k_e from the cloud bottom CBH to the cloud top CTH. When the cloud layers are assumed to be vertically homogeneous, the geometric thickness ΔZ can be represented by the following equation:

$$\Delta Z = CTH - CBH \approx \tau / k_e \tag{2}$$

For water clouds, the extinction coefficient k_e is the total extinction cross section for particles in a unit volume. In the proposed method, we use the modified Gamma distribution [CLA74] with broadness 2 for describing the particle size distribution. Therefore, The extinction coefficient k_e is related to the effective particle radius r_e as follows:

$$k_e = 0.75 N_0 \pi r_e^2 \tag{3}$$

where N_0 denotes the total density of particles and $N_0 \approx 60 cm^{-3}$ within the water clouds (cumulus clouds and stratus clouds) above the sea [Che05].

For ice clouds, the effective particle size, similar to the effective radius for water clouds, has different definitions. One of the definitions is from the work of Foot [Foo88] and another D_e^{FL} is given by Fu and Liou [QL93]. When the length of ice crystal is equal to its width, we observe that $D_e^{FL} = 1.1 D_e^{FT}$. The extinction in visible spectrum is then related to the effective size D_e^{FT} as follows [QL93]:

$$k_e = IWC(a_0 + a_1/(1.1 D_e^{FT}) \tag{4}$$

where a_0, a_1 are coefficients, and IWC denotes the ice water content which can be parameterized as the function of the temperature [OTL*03].

From Eq.(2) to (4), the optical thickness, the effective radius r_e (water clouds), and the effective size D_e^{FT} (ice clouds) become our new targets for estimating the geometric thickness and the extinction. In order to determine these parameters, we resort to the reflection function of a plane-parallel cloud layer which models the ratio of the reflected intensity to the incident solar flux density.

When the optical thickness of the cloud layer is sufficiently large, the analytical equations for reflection functions [KR04] can be written as follows:

$$\Re_{vis} = \Re_{vis}(\tau_{vis}, g_{vis}, \omega_{vis}, v, v_0, \phi) \tag{5}$$

$$\Re_{mwir} = \Re_{mwir}(\tau_{mwir}, g_{mwir}, \omega_{mwir}, v, v_0, \phi) \tag{6}$$

where $\Re_i$ is the reflection function, τ_i the optical thickness, g_i the asymmetry parameter, ω_i the single scattering albedo ($i = ir, mwir$), v the satellite zenith angle, v_0 the solar zenith angle, and ϕ represents the relative azimuth. For simplicity, we omit the detailed forms of the two equations. In addition, the optical thickness in MWIR spectrum is related to the optical thickness in the VIS spectrum [NK11]:

$$\frac{\tau_{mwir}}{\tau_{vis}} = (\frac{\lambda_{mwir}}{\lambda_{vis}})^{2/3} \frac{1.1 + \zeta_{mwir}^{2/3}}{1.1 + \zeta_{vis}^{2/3}} \tag{7}$$

where $\zeta_i = 2\pi r_e/\lambda_i$, λ_i is the central wavelength.

For water clouds, the asymmetry parameter and the single scattering albedo can be parameterized in terms of the efficient radius for 24 wavebands [Sli89]:

$$\omega_i = 1 - c_i - d_i r_e \tag{8}$$

$$g_i = e_i + f_i r_e \tag{9}$$

where c_i, d_i, e_i, f_i are the coefficients, and i denotes the waveband. The above equations from (5) to (9) form a complete set of governing equations for the solution of three unknown variables: $\tau_{vis}, \tau_{mwir}, r_e$. To solve these equations, the measured reflectance recorded in VIS image is directly assigned to $\Re_{vis}$. However, during daytime, the MWIR radiance contains both thermal emission and solar reflection, the reflectance $\Re_{mwir}$ is obtained by removing the thermal emission part [LHG*06].

For ice clouds, the optical thickness and the asymmetry parameter are both independent of the wavelength. In particular, $g_{vis} = g_{mwir} \approx 0.74, \tau_{vis} = \tau_{mwir}$, and $\omega_{vis} = 1.0$ [KN05]. Therefore, there are only two unknowns (τ_{vis} and ω_{mwir}) in the two equations Eqs.(5) and (6), so the optical thickness τ_{vis} and the single scattering albedo ω_{mwir} can be solved. Furthermore, D_e^{FT} can be represented as the function of single scattering albedo ω_{mwir} [KN05]:

$$D_e^{FT} = f(\omega_{mwir}) \tag{10}$$

Until now, we have obtained the geometry thickness and extinction of water clouds and ice clouds. However, as the analytical form of the reflection function is not fit to the optically thin cirrus clouds, the geometric thickness of the thin cirrus is estimated by using the empirical equation [PJD87]. From the three temperatures of the ground, the clouds, and the IR1 image, we can estimate the emissivity and then compute the optical thickness τ_{vis} [PKY93]. Finally, the extinction k_e of thin cirrus can be computed:

$$k_e = \tau_{vis}/\Delta Z \tag{11}$$

In Fig. 2(d), the pixel intensity indicates the thickness in that more brighter, more thicker. We can easily observe that cumulonimbus have the biggest thickness while thin cirrus clouds and part of water clouds have smaller thickness. Especially, the distribution of thickness is very similar to that of grey intensity in the VIS image (a). Since the grey intensity of the VIS image reflects approximately the thickness of the cloud, the estimated thickness is rational.

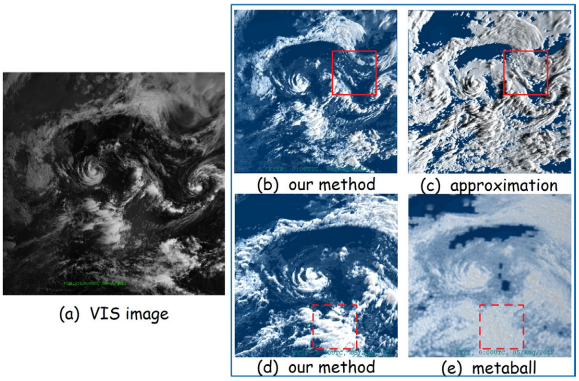

Figure 3: *Contrast with other methods. (a) the input visible image. (b) and (d) our results. (c) approximation scheme [DYN09]. (e) metaball [DNYO98].*

Once CTH, CBH and k_e for each cloud pixel are available, we construct a regular volume representation and a particle based representation for rendering. For the regular volume sampling, the earth surface is assumed to be flat and the extinction of the sample located between the cloud top and the cloud bottom is set to that of the cloud pixel. Particle sampling is similar to the regular volume sampling with the exception that a particle is placed at a specific position by taking into account of the earth curvature. For cloud rendering, we use the typical two-pass methods [Har05].

4. Results

Our work is performed on a PC with an i5-2300 Intel(R) Core(TM) 2.8GHz CPU. The size of the input images is 512×512 with a spatial resolution of 15km $\times$ 15 km and can be downloaded freely at *http://nsmc.cma.gov.cn*. These images were recorded between 0:00 and 6:30 UTC on 5th August 2012. During this time, a typhoon named 'Haikui' was formed above Chinese southeast coast. The resolution of the extinction volume is $512 \times 512 \times 256$ and the number of particles are about 40,000. For each frame, the time cost of the modeling process is nearly 4 seconds. Due to the low distance in height (20km) compared to the width and breadth (512×15km) of large scale clouds, we scale up the height in order to give a better depth perception.

In Fig. 3, we compare our method with other two methods. The first method is an approximation solution similar to the one described in [DYN09]. The red squares show that our method (b) can reflect the local thickness distribution better than the approximation method (c). Note that the shading of our image (b) is similar to that of the VIS image (a). It is not easy to achieve the effect by trivially adjust-

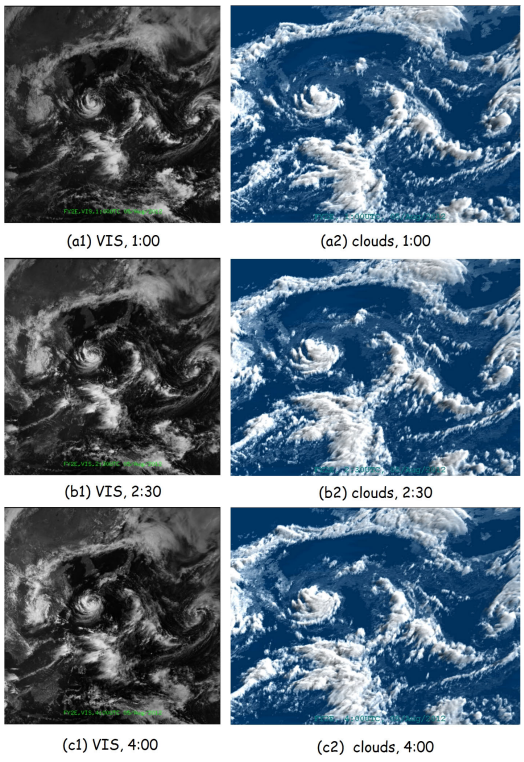

Figure 4: *Three clouds modeled from multi-spectral images at 1:00,2:30,4:00 UTC.*

ing thickness distribution or cloud density. In (e), the cloud is generated according to the method described in Dobashi et al. [DNYO98]. We can observe that the cloudless region is easily covered by these metaballs unless very small metaballs are used. In addition, the resulting surface tends to be a little flat (dot square in (e)). In contrast, our method can generate clouds with distinct geometric structures as shown in (b) and (d).

In Fig. 4, we present a time series of clouds, corresponding to the satellite images at 1:00, 2:30 and 4:00 UTC. In Fig. 5, we render the clouds from the satellite images at 0:00UTC in different views and the visible image is shown in Fig. 3(a). In addition, the result for two light conditions (daytime and evening) is shown in Fig. 1. From these results, the 3D geometric structure of the clouds can be easily observed. Since the structures of the clouds are key to atmospheric research, the above results are appropriate for the professional applications. To integrate our clouds to more realistic environment, we use particle system to visualize the shape of the clouds on the earth as shown in Fig. 6.

5. Conclusion and future work

In this paper, based on cloud property retrieval theory, the proposed method takes major simplifications to the weather model and creates a processing chain that takes multi-spectral satellite images as the input and delivers a meaningful and fast 3D visualization of the large scale clouds.

However, there exists a few limitations. First, VIS images are only available at daytime, and the proposed method thus can not model the cloud at night. Second, a few assumptions are used in our method, which means that our method is just an approximate solution to the reconstruction of 3D clouds. An actual evaluation may be required although it is quite complex given the nature of the data. Third, low resolution image data are used to construct clouds, which yield an unsatisfactory sight when the viewpoint is near to the clouds.

Based on the current version of our work, we suggest two possible directions to further improve it :

i. A statistical temperature-altitude table can be used to accurately locate the cloud top.
ii. Higher resolution images (MODIS) should be utilized to represent detailed cloud scene.

Acknowledgments

This paper is supported by National Natural Science Foundation of China (No. 61170186,61073078, 61272348), Beijing Natural Science Foundation (Researches on Human Body Segmentation Methods in Natural Environment based on Computer Vision) and Ph.D. Program Foundation of Ministry of Education of China (No. 20111102110018). We would like to thank the anonymous reviewers for helpful comments, Professor Jiming Sun for useful discussions on cloud physics, and Chuanjie Jing for the video.

References

[BN04] BOUTHORS A., NEYRET F.: Modeling clouds shape. In *Eurographics (short papers)* (august 2004). 2

[Che05] CHEN W.: *Satellite meteorology (in chinese)*. China Meteorological Press, Beijing, China, 2005. 3

[CLA74] CLARK T.: A study in cloud phase parameterization using the gamma distribution. *J. Atmos. Sci. 31*, 1 (1974), 142–155. 3

[DIO*12] DOBASHI Y., IWASAKI W., ONO A., YAMAMOTO T., YUE Y., NISHITA T.: An inverse problem approach for automatically adjusting the parameters for rendering clouds using photographs. *ACM Trans. Graph. 31*, 6 (2012), 145:1–145:10. 2

[DKNY08] DOBASHI Y., KUSUMOTO K., NISHITA T., YAMAMOTO T.: Feedback control of cumuliform cloud formation based on computational fluid dynamics. *ACM Trans. Graph. 27*, 3 (Aug. 2008). 2

[DNYO98] DOBASHI Y., NISHITA T., YAMASHITA H., OKITA T.: Modeling of clouds from satellite images using metaballs. In *Proceedings of the 6th Pacific Conference on Computer Graphics and Applications* (1998), pp. 53–60. 2, 4, 5

[DSY10] DOBASHI Y., SHINZO Y., YAMAMOTO T.: Modeling of clouds from a single photograph. *Computer Graphics Forum 29*, 7 (2010), 2083–2090. 2

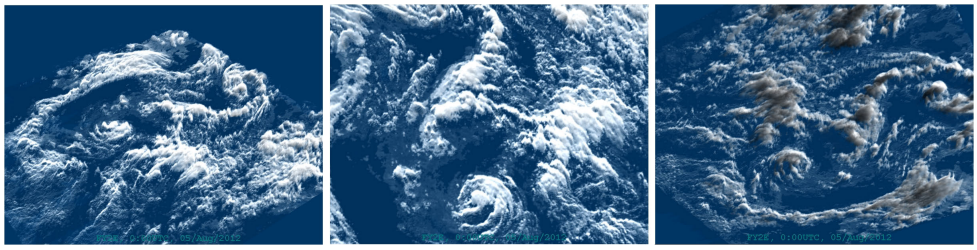

Figure 5: *Clouds at 0:00UTC are rendered in multiple views.*

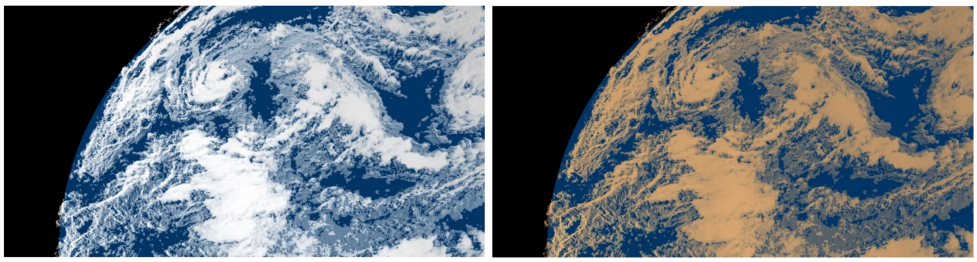

(a) particle sampling (daytime) (b) particle sampling (evening)

Figure 6: *Clouds at 0:00UTC are represented as particle system.*

[DYN09] DOBASHI Y., YAMAMOTO T., NISHITA T.: Interactive and realistic visualization system for earth-scale clouds. In *Pacific graphics 2009(poster paper)* (2009). 2, 4

[Ebe] EBERT D. S.: Volumetric modeling with implicit functions: a cloud is born. In *ACM SIGGRAPH 97 Visual Proceedings*. 2

[Foo88] FOOT J.: Some observations of the optical properties of clouds. ii: Cirrus. *Quarterly Journal of the Royal Meteorological Society 114*, 479 (1988), 145–164. 3

[Gar85] GARDNER G. Y.: Visual simulation of clouds. *SIGGRAPH Comput. Graph. 19*, 3 (July 1985), 297–304. 2

[Har05] HARRIS M. J.: Real-time cloud simulation and rendering. In *ACM SIGGRAPH 2005 Courses* (2005). 2, 4

[Ino87] INOUE T.: A cloud type classification with noaa 7 split-window measurements. *Journal of Geophysical Research 92*, D4 (1987), 3991–4000. 2

[KN05] KOKHANOVSKY A., NAUSS T.: Satellite based retrieval of ice cloud properties using a semianalytical algorithm. *Journal of geophysical research 110*, D19 (2005). 4

[KR04] KOKHANOVSKY A. A., ROZANOV V. V.: Simple approximate solutions of the radiative transfer equation for a cloudy atmosphere. In *Proceedings of SPIE* (2004), vol. 5571, pp. 86–93. 2, 3

[LHG*06] LINDSEY D. T., HILLGER D. W., GRASSO L., KNAFF J. A., DOSTALEK J. F.: Goes climatology and analysis of thunderstorms with enhanced 3.9-μ m reflectivity. *Monthly weather review 134*, 9 (2006), 2342–2353. 4

[MYND01] MIYAZAKI R., YOSHIDA S., NISHITA T., DOBASHI Y.: A method for modeling clouds based on atmospheric fluid dynamics. In *Proceedings of the 9th Pacific Conference on Computer Graphics and Applications* (2001), pp. 363–372. 2

[NK11] NAUSS T., KOKHANOVSKY A. A.: Retrieval of warm cloud optical properties using simple approximations. *Remote Sensing of Environment 115*, 6 (2011), 1317–1325. 4

[OTL*03] OU S.-C., TAKANO Y., LIOU K., HIGGINS G. J., GEORGE A., SLONAKER R.: Remote sensing of cirrus cloud optical thickness and effective particle size for the national polar-orbiting operational environmental satellite system visible/infrared imager radiometer suite: sensitivity to instrument noise and uncertainties in environmental parameters. *Applied optics 42*, 36 (2003), 7202–7214. 3

[PJD87] PLATT C., J.C. S., DILLEY A.: Remote sounding of high clouds. part vi:optical properites of midlatitude and tropical cirrus. *J. Atmos. Sci. 44* (1987), 729–747. 4

[PKY93] P. M., K. L., Y. T.: Inference of cirrus cloud properties using satellite-observed visible and infrared radiances. part i: Parameterization of radiance fields. *J. Atmos. Sci. 50* (1993), 1279–1304. 4

[QL93] QIANG F., LIOU K.: Parameterization of radiative properties of cirrus clouds. *J Atmos Sci 50*, 13 (1993), 2008–2025. 3

[REHL03] RILEY K., EBERT D., HANSEN C., LEVIT J.: Visually accurate multi-field weather visualization. In *Proceedings of the 14th IEEE Visualization 2003* (2003), pp. 279–286. 2

[Sli89] SLINGO A.: A gcm parameterization for the shortwave radiative properties of water clouds. *Journal of Atmospheric Sciences 46* (1989), 1419–1427. 4

[Sze82] SZEJWACH G.: Determination of semi-transparent cirrus cloud temperature from infrared radiances: Application to meteosat. *Journal of Applied Meteorology 21*, 3 (1982), 384–393. 3

[WBC08] WITHER J., BOUTHORS A., CANI M.-P.: Rapid sketch modeling of clouds. In *Eurographics Workshop on Sketch-Based Interfaces and Modeling (SBIM)* (2008), Eurographics. 2

[XZYZ08] XU J., ZHANG W., YANG J., ZHAO L.: *User guide for products and data formats of FY2 (in chinese)*. China Meteorological Press, Beijing, China, 2008. 3